Finite Element Analysis of Human Clavicle Bone

Author: Travis Jones

Advisor: Dr. Rebecca Dupaix

The Ohio State University

May 2012

Abstract

Each year there are thousands of clavicle fractures as a result of the three-point belt system in car crashes. Although a lot of testing is put into the safety of passengers during automobile crashes there is still some uncertainty concerning the realistic response of the anthropomorphic testing devices (ATDs) use to represent the passengers. This study looked specifically to create a more accurate representation of the human clavicle's response during a collision. The geometry of the clavicle was created from converting CT-scans of subjects into 3D-models. The clavicle was constrained by using spring elements in a finite element program in order to represent the ligaments which constrain the clavicle in the human body. Although there have been other studies done which have created finite elements tests of the clavicle. These were only made to verify three-point bending test results and used simplifications of the boundary conditions. Simulations were run to determine if load position was a factor in clavicle fractures. Using the model created it was found that the peak stress occurs when the belt load is centrally located on the clavicle. The stress decreases slightly as the load is moved laterally (toward the shoulder) and decreases dramatically as the load is moved medially (toward the neck). The process and model developed in this study could help in the creation of more accurate bone representations in ATDs for crash testing purposes.

Acknowledgements

I would like to thank Dr. Rebecca Dupaix for giving me the opportunity to work on this project

I would also like to thank Jason Stammen for making this research available and his guidance throughout the project

Table of Contents

List of Figures

List of Tables

Chapter 1

1.1 Focus of Thesis

Clavicle injuries are a common injury in car accidents. In a study done by Kemper et al. they found through the National Automotive Sampling System's Crashworthiness Data System (NASS-CDS) that over 9,700 three-point belt-restrained occupants incur a clavicle fracture every year. The shoulder belt was found to be the cause of over 90% of these fractures for frontal automotive impacts. These clavicle injuries and other injuries caused by seatbelts are referred to as "seat belt syndrome." The main focus of this paper is to develop a realistic model of the human clavicle that would respond just like a real clavicle would in an accident, independent of load direction. Three clavicle computer tomography (CT) scans will be modeled in finite element analysis software. These models will eventually have dynamic loads applied to them and have the results of the finite element analysis compared to that of results from actual car crash data of individuals of similar age. This paper will solely focus on the creation of the clavicle model and the boundary conditions and variables that could affect the outcome of the simulations. The future work will be discussed in Chapter 4 which will involve applying dynamic force data determined from car crash simulations and comparing them with the outcome of the car accident to determine fracture tolerances.

1.2 Literature Overview

The material properties of the clavicle bone in our model will be based on data in the research literature. There have been many studies on the properties of bone in general but there has not been much research as far as the analysis of the clavicle bone. The few studies that have been done involved three-point bend tests of adult clavicles in either quasi-static or dynamic loading. All of these studies used different boundary conditions to secure their clavicles during the three-point bending tests. Bolte et al. conducted three-point bending tests on six adult clavicle bones at an impact rate of 0.5mm/s. They did

not specify their boundary conditions. Kemper et al. tested ten adult clavicles at an impact rate of 152mm/s. They used a pinned-simply supported set-up. Proubasta et al. conducted three-point bending test on five adult clavicles at an impact rate of 0.5mm/s. They used a fixed-fixed boundary condition. Untaroiu et al. conducted three-point bending test on six human post mortem subjects with an impact rate of 1mm/s (quasi-static) and 1m/s (dynamic). They used a pinned-pinned boundary condition. A finite element model was also used and optimized to obtain an elastic modulus of 8.1GPa. In another study done by Kemper et al. a dynamic test was performed on the clavicle and a Young's modulus of 20.8±5.7GPa was determined. This differs greatly from that of the Young's modulus found in the study done by Untaroiu et al. The difficulty in assigning material properties to cortical bone is in its non-isotropic properties. Cortical bone is much stiffer in compression than it is in tension and has strain-dependent properties in the plastic region of deformation (Skalak & Chien, 1987). There is not a lot of data available on the material properties of pediatric clavicles. This is due in large part to the ethical boundaries of testing pediatric samples.

For the purposes of this research the material properties of the clavicle would have to be estimated based on relationships between age and bone strength. Several studies have determined linear relationships between the Young's modulus of bone and the bone mineral density (BMD) (Nuckley & Ching) (Vinz, 1972). There was also found to be a linear relationship between the bone mineral content and age of the subject. This helps to explain the trends in bone strength changing with age found in several other studies (Currey & Butler, The Mechanical Properties of Bone Tissue in Children, 1975) (Vinz, 1972). Currey and Butler found that the modulus of elasticity and bending strength both increase with age until about 30 years of age and then decrease thereafter. The study done by Vinz investigated the material properties of bone samples of age zero to eighty-five years. He found that the tensile strength and modulus of elasticity increased from age zero to age forty and then began to fall. He also stated that there was more plastic deformation in the younger samples. These findings were considered when applying different material properties to the clavicle models. However as no dynamic tests were applied during this study, only the elastic property of the clavicle was considered.

The three CT scans that were provided for the initial development of the modeling process were those of a 21 year old male, 53 year old female, and 65 year old female. For future work the Children's Hospital of Philadelphia will be providing CT scans of pediatric clavicles. This will allow us to further our understanding of the differences between the geometries of an adult and child clavicle. With the advent of software that can convert CT scans into finite element models, computer models have become increasingly realistic. The CT scans were converted into a 3-D model using 3D-Doctor. SolidWorks was then used to convert the model exported from 3D-Doctor into a workable model for the finite element analysis. ANSYS was used for all of the finite element analysis of the clavicle. The study done by Untaroiu et al. they used a finite element software LS-Dyna to perform their simulations. In the future work section other programs will be discussed for possible alternatives to that being used in this study.

1.3 Overall Research

The overall research project being worked on by the School of Biomedical Science here at The Ohio State University is to better understand the response of the pediatric torso's response to three-point belt loading. The goal is to develop a better model of the torso for children for car crash testing. Arbogast et al. stated that there is no current pediatric anthropomorphic testing device (ATD) that can accurately quantify the abdominal response to belt loading. This paper focuses on a small part of the overall research which is creating a more accurate model of the clavicle bone. Future work will include expanding the analysis to other parts of the torso.

1.4 Overview of Thesis

The rest of the paper will explain in detail the processes of developing the final model that can be used for simulations. Chapter 2 will explain how the CT scans were converted into the solid model that was used in the finite element analysis. Chapter 3 will present all of the boundary conditions and variables that were considered in setting up the model. The different aspects that were considered were

how the model was fixed, the orientation of the clavicle, and load location. The chapter will include the process of setting up the model as well as results from different tests to confirm the different boundary conditions. Chapter 4 will give a summary of the research and where this work will take us in the future.

Chapter 2

2.1 Obtaining Clavicle Geometry

In order to assess the effect of belt loading in physiological realistic clavicles, we need a method to procure and import the geometry from a real human subject. The geometry would be taken from CT-scans of a human cadaver. A CT scan consists of multiple images that make up a stack of images that are essentially slices of the object being scanned. Figure 2 shows an example of one of the image slices from the CT scan of the 21 year old male. The sections in these images need to be taken and converted into a working finite element model. Several software products will be required to convert the CT images into an accurate 3D model. Figure 1 shows the order and names of the software that will be used in this process.

Figure 1: Flow Chart of Software to be used

The first step is to use 3D-Doctor to remove the bones that are of interest in our study. The program uses a thresholding technique to differentiate the bone from the rest of the body by looking at the degree in variation of the light intensity of each pixel. By adjusting the threshold of light intensity one can select the cortical bone and separate it from the surrounding material.

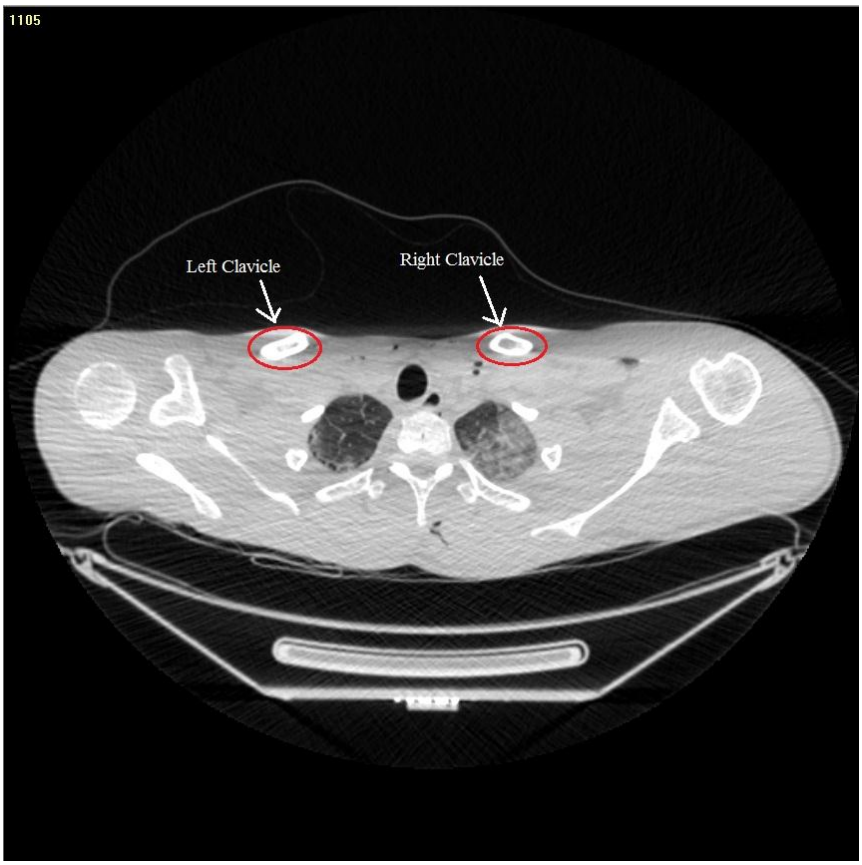

Figure 2: CT Image Slice with Clavicle Labels

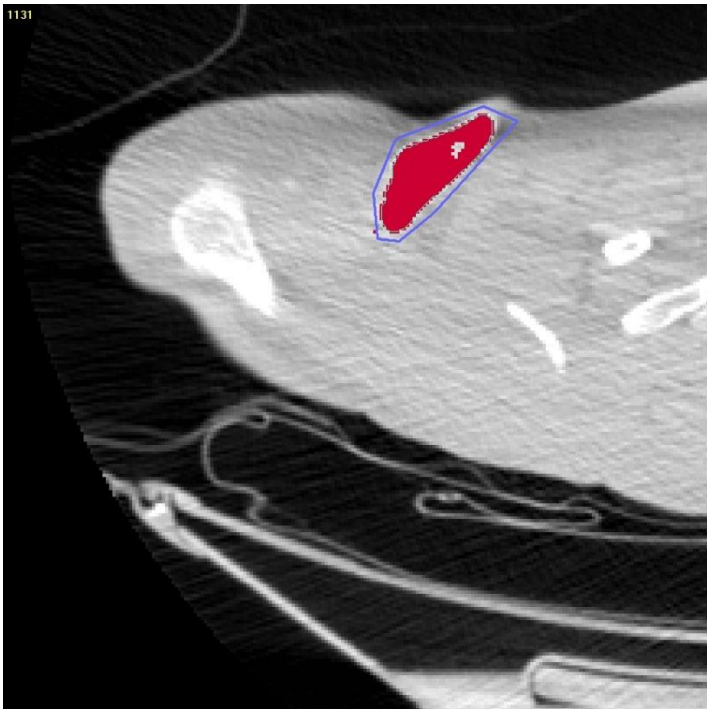

Figure 3: Example of Thresholding Technique of a Section of the Left Clavicle

This is done for each image that contains a section of the clavicle bone. Figure 3 shows an example of what the section of bone looks like when it has been highlighted through the thresholding technique. This figure shows that the resolution of the image plays a large role in the initial smoothness of the model. There are very jagged edges on the highlighted section of bone due to the discrete size of the pixels. If the pixels were infinitely small it would be a smooth surface but since they have a defined size it creates rough edges. Once all of the sections have been identified a surface model is created. An example of what the model initially looks like is shown in Figure 4. The layers from each image slice can clearly be seen. This is because of the discrete number of images for the entire bone. Just as with the pixels, if there had been in an infinite amount of image slices the surface would be much smoother but since there was a set number of images it make it harder to create a smooth model. This is undesirable for the model to be used as this is not representable of the actual clavicle. It is possible to simplify and smooth the model in 3D-Doctor but for my study I chose to do all the smoothing and simplifying in SolidWorks.

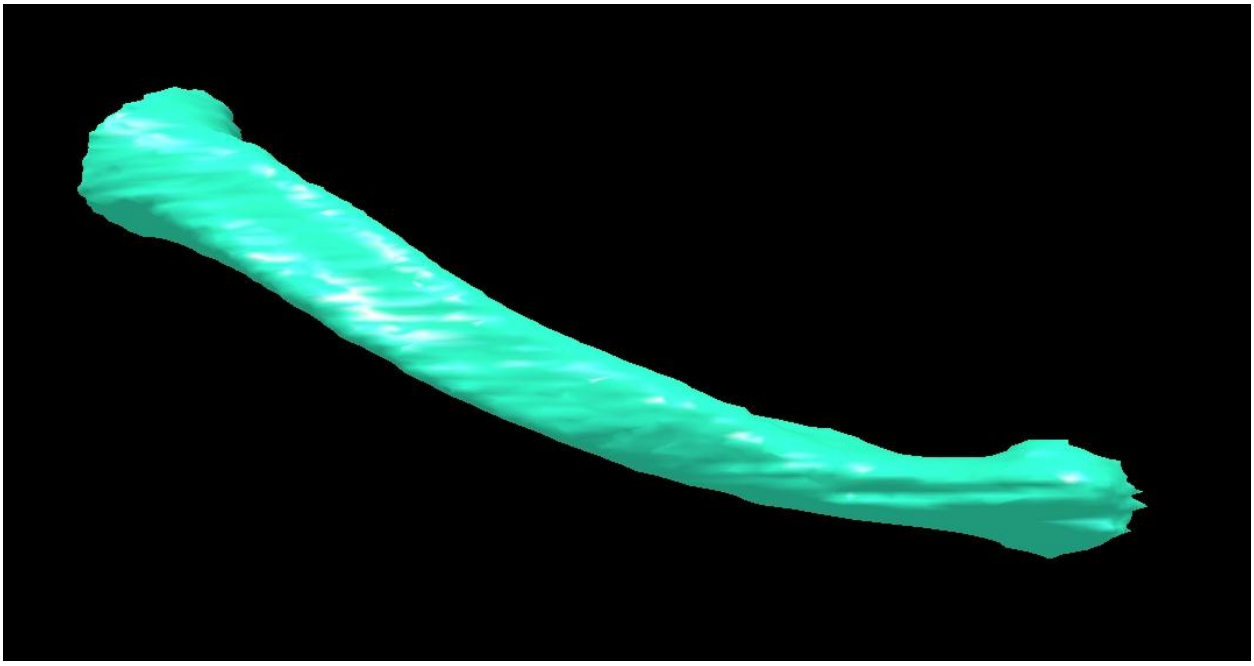

Figure 4: Initial Simple Surface Model Side View

2.2 Finalizing Model in SolidWorks

The models were exported as stereo lithographic files (STLs) from 3D-Doctor and imported into SolidWorks. Using SolidWorks' add-in ScanTo3D the meshes were simplified and smoothed and then exported as an initial graphics exchange specification file (IGES). The benefit of simplifying a model is to reduce the size of the file which reduces the computation time when it comes to the simulation. This is most noticeable when a model is reduced from thousands of nodes to only a couple hundred. There is an issue with simplifying too much however. If the model is reduced too much some of the actual parts of the model can be lost. The key is to find balance between getting the model to a reasonable number of nodes while maintaining the realistic shape. Figure 5 through Figure 9 shows the result of simplifying the model at different percentage reductions. There is not a noticeable difference between 60 and 70% however it is clear to the naked eye that the model is starting to lose substance at reductions greater than 90%.

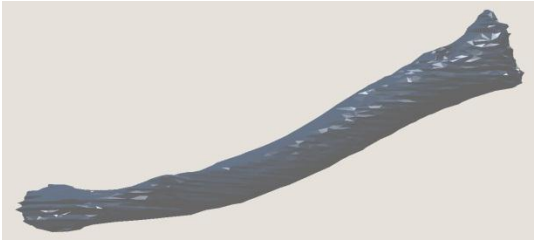

Figure 5: 60% Simplified

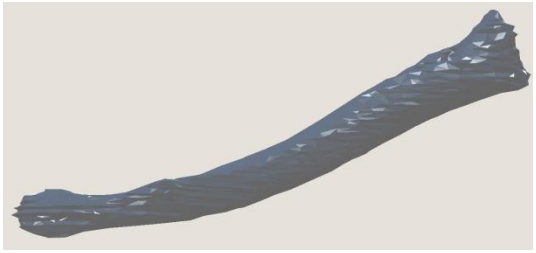

Figure 6: 70% Simplified

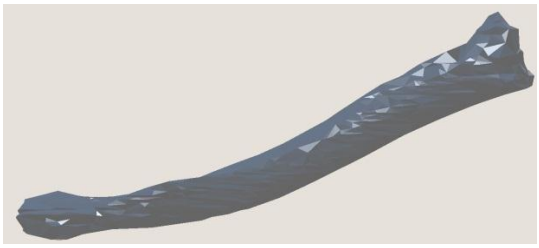

Figure 7: 80% Simplified

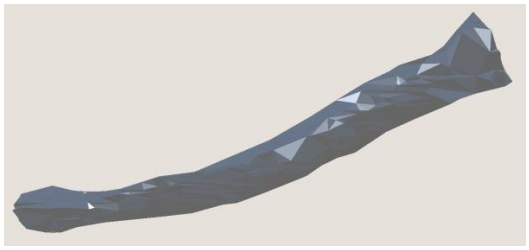

Figure 8: 90% Simplified

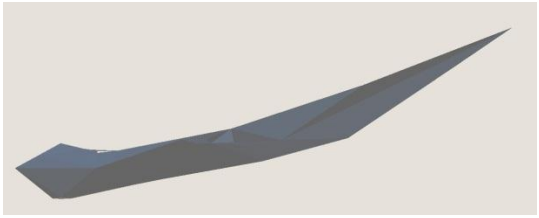

Figure 9: 99% Simplified

For the models in this study 50% simplification was chosen. This percentage was selected as it reduced the number of nodes to a reasonable amount while not removing any geometry that is part of the bone.

The next step involved smoothing the model to remove any stress concentrations that may have been the result of discrete pixel sizes of the CT images in 3D-Doctor. Actual bone does not have a jagged surface and this characteristic of the model is a result of the poor resolution of the CT images as stated before. We want a realistic model as possible and any extra material that isn't an actual part of the bone would result in unrealistic results. Such surface errors could also lead to stress concentration factors causing the stresses to be unrealistically high. Smoothing the model also makes it easier to create a mesh and there is a far less chance there will be any face or gap errors. Unlike the nodal simplification, the smoothing process does not dramatically remove material and the difference between levels of smoothness is very minimal. Figure 10 shows the Sternoclavicular end of the original model without any

smoothing. Figure 11 shows the model with the minimum amount of smoothing. Figure 12 shows the model with maximum smoothness applied. Although there is a major difference between the no smoothing and the minimum smoothing, there is almost no change at all between the minimum and maximum smoothed models.

Figure 10: Sternoclavicular End with No Smoothing

Figure 11: Sternoclavicular End with Minimum Smoothing

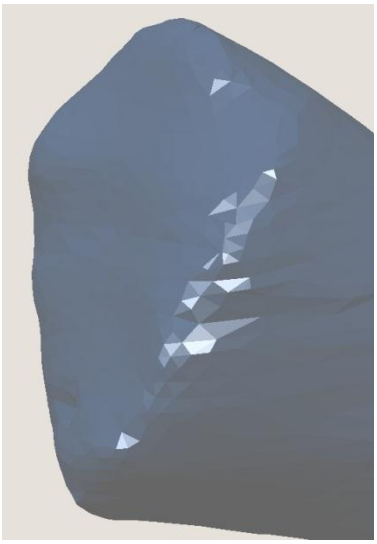

Figure 12: Sternoclavicular End with Maximum Smoothing

2.3 Difficulties in Model Creation

There were a lot of errors in moving the model from SolidWorks into ANSYS due to the clavicles complicated geometry. Due to this it was very hard to try and develop multiple models and the simulations done were limited to only a single model. This model used 50% simplification and the maximum smoothing.

2.4 Lofted Model Creation

Chapter 3

3.1 Boundary Conditions

Once a model has been determined for a finite element analysis the next step is to determine the boundary conditions that will be applied to the model. For the clavicle the boundary conditions will

attempt to recreate the same support structure that the ligaments of the body perform. The simplest way to do this is to constrain specific nodes on the actual clavicle by assuming that the ligaments would act as rigid supports. The question that was raised however is how many nodes would be needed to secure the ends of the clavicle. The more nodes constrained the less flexibility there is while the fewer nodes there are the more unrealistic the stress levels can become.

Different combinations of nodal constraints were tested with a standard load of 200N. The reason that a different number of nodes were selected is because there is no way of constraining the rotation of a 3D model. The only way to do this is to constrain the nodes in such a way that the model can no longer rotate around a certain axis. By constraining fewer nodes the model is allowed to rotate much more freely. Table 1 shows the results of these trials. The max stress value was recorded along with the location.

Table 1: Nodal Constraint Test Results

Sternoclavicular Joint Boundary Condition	Acromioclavicular Joint Boundary Condition	Maximum Stress
1 Node	3 Node	788
3 Node	1 Node	287
1 Node	7 Node	575
1 Node	20 Node	409.8
1 Node	50 Node	238.7
1 Node	Cantilevered*	179
7 Node	Cantilevered	138.1
20 Node	Cantilevered	83.2
Cantilevered	1 Node	178.2
Cantilevered	7 Node	251.5
Cantilevered	20 Node	205
Cantilevered	Cantilevered	75.5

*Cantilevered means there were enough nodes that the end acted like it was cantilevered

These results give a few key notes of interest. The first of which is that constraining too few nodes can lead to extreme stress concentrations at the points of constraint. Figure 13 shows an example of this. The second is that the maximum stress does not change as dramatically with the variation in the Sternoclavicular constraint as it does with the variation in Acromioclavicular constraint.

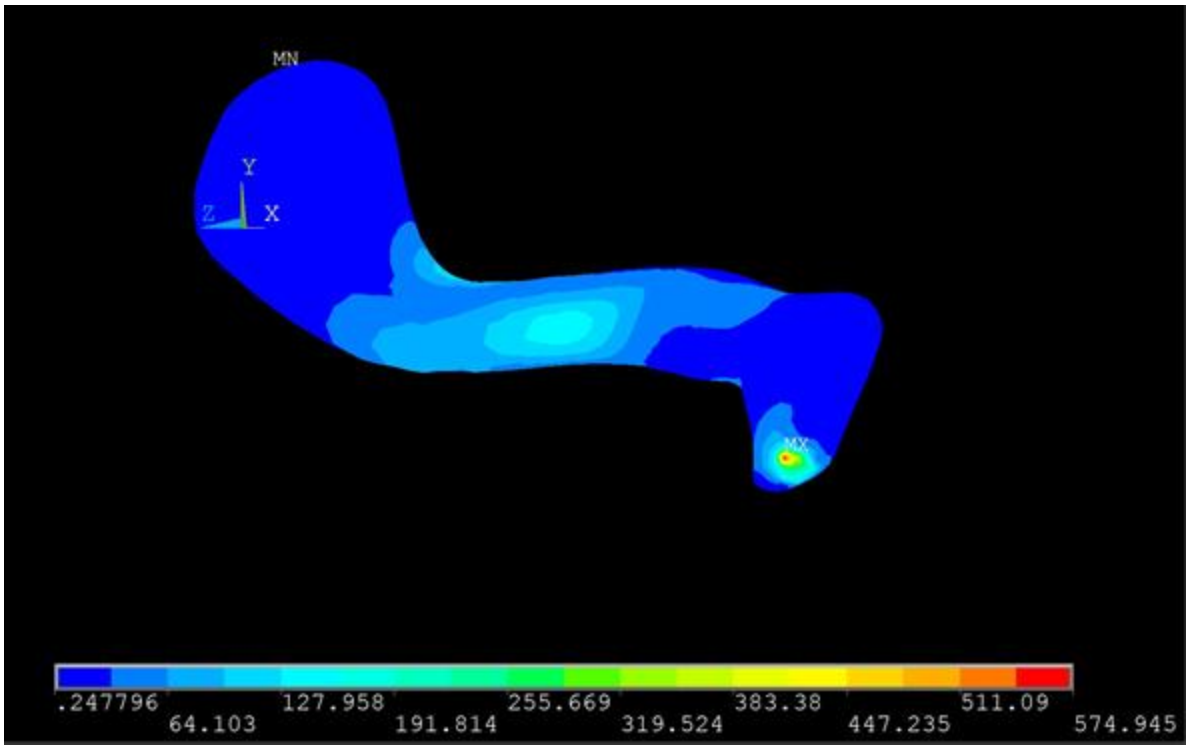

Figure 13: Single Node Constraint on Acromioclavicular Joint

In order to better represent the actual clavicle and how it is supported in the human body, spring elements were used to imitate ligaments. Figure 14 shows an anatomical picture of the clavicle with the ligaments labeled. Figure 15 shows the model with the spring elements in place and the corresponding ligaments that they are representing.

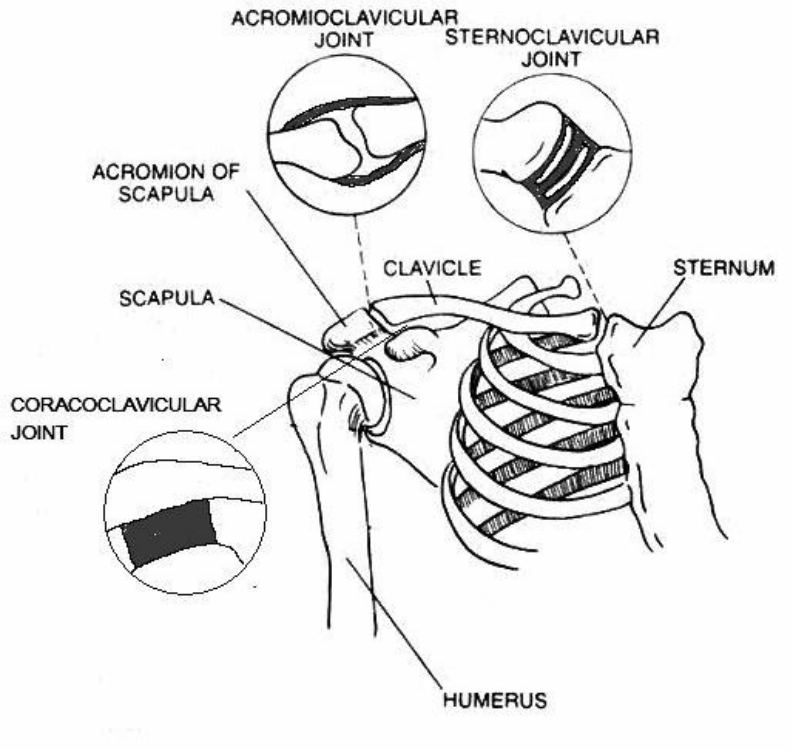

Figure 14: Anatomical Diagram of Clavicle

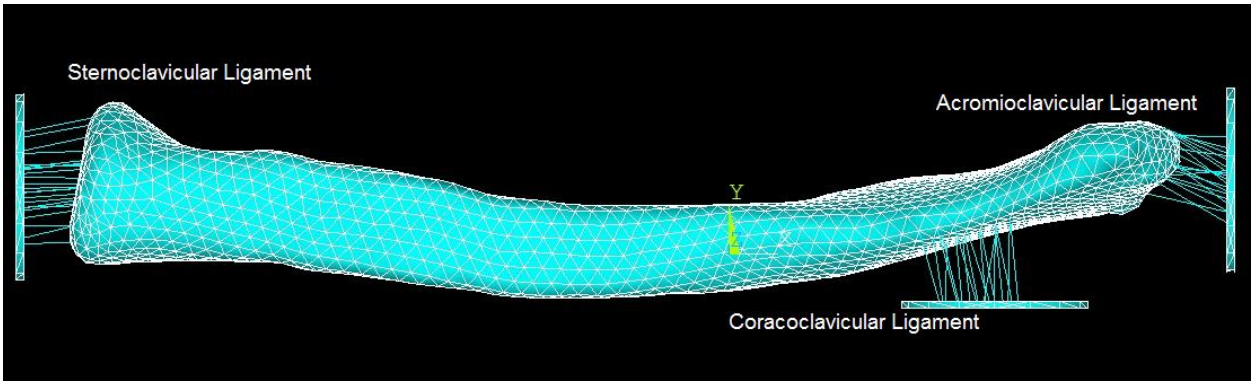

Figure 15: Finite Element Model with Ligament Constraints

After the model was created a few things were pointed out about the accuracy of the model in an anatomical sense. The first and most important of which is that the clavicle is upside down in the constraints. The Coracoclavicular ligament should be on the opposite side of the bone. The other aspect of the model that needs to change is the structure of the Acromioclavicular ligament and Sternoclavicular ligament. The Acromioclavicular ligament is actually attached along the top side of the

clavicle in an arc pattern. The Sternoclavicular ligament should also be changed so that it is not a solid ligament structure but instead a ring that goes around the edge of the Sternoclavicular end of the bone.

3.2 Load Location

Once the model was constrained the next step was to test the effect of load location on the clavicle. Of all clavicle fractures that occur each year, a high percentage of them are pediatric. As children have much more flexible bones and a smaller mass it would seem like they would experience lower stress in their bones. A key variable however is that the belt is much closer to the neck than for an adult. This fact in combination with the abnormal geometry of the clavicle could be resulting in higher stresses. Three simulations were done where the load was moved in one inch increments (25.4mm) from the Sternoclavicular end to the Acromioclavicular end. The load was a distributed load that represented a belt load about three inches in width. The value of the load was arbitrarily defined with the only requirement that it kept the bone within the elastic region of deformation. Figure 17 shows the stress distribution when the load is placed 38mm (~1.5in) from the Sternoclavicular end. Figure 18 shows the back view of the same stress plot. An interesting note to make is that the maximum stress occurs on the back side of the clavicle. This is actually representative of real life but for a different reason, as cortical bone is much weaker in tension than it is in compression. The material properties of the simulation are limited and cannot properly represent this characteristic of cortical bone. This means that the higher stress that is apparent on the back side of the clavicle in these simulations is a result of the geometry of the bone. The location of the maximum stress is also of importance. The maximum stress occurs at the middle third of its length which is characteristic of clavicle fractures in real life.

Figure 16 shows the maximum stress and how it varies with where the load is being applied. As can be seen the stress actually drops off as the load is moved closer toward the Sternoclavicular end or in other words towards the neck.

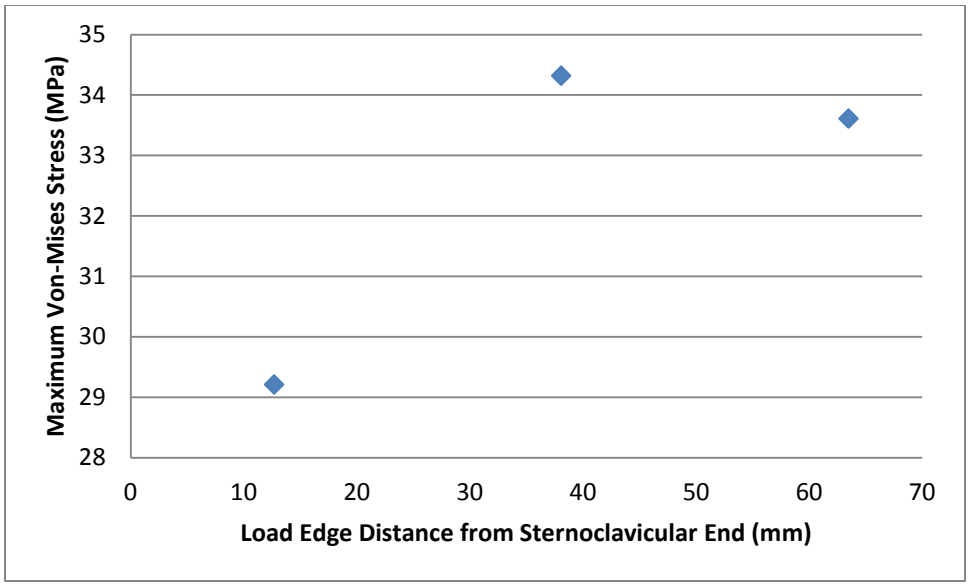

Figure 16: Plot of Maximum Stress vs. Load Location

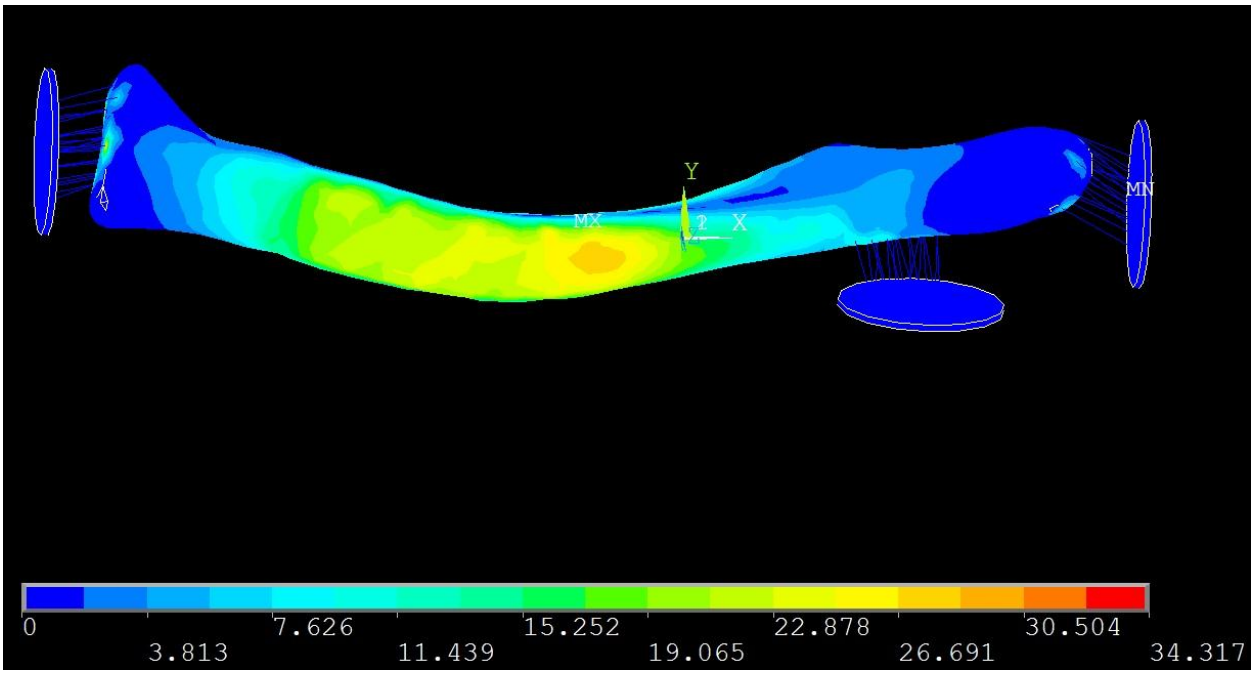

Figure 17: Front View of Stress Distribution of 135N Load Applied 38 mm from Sternoclavicular End

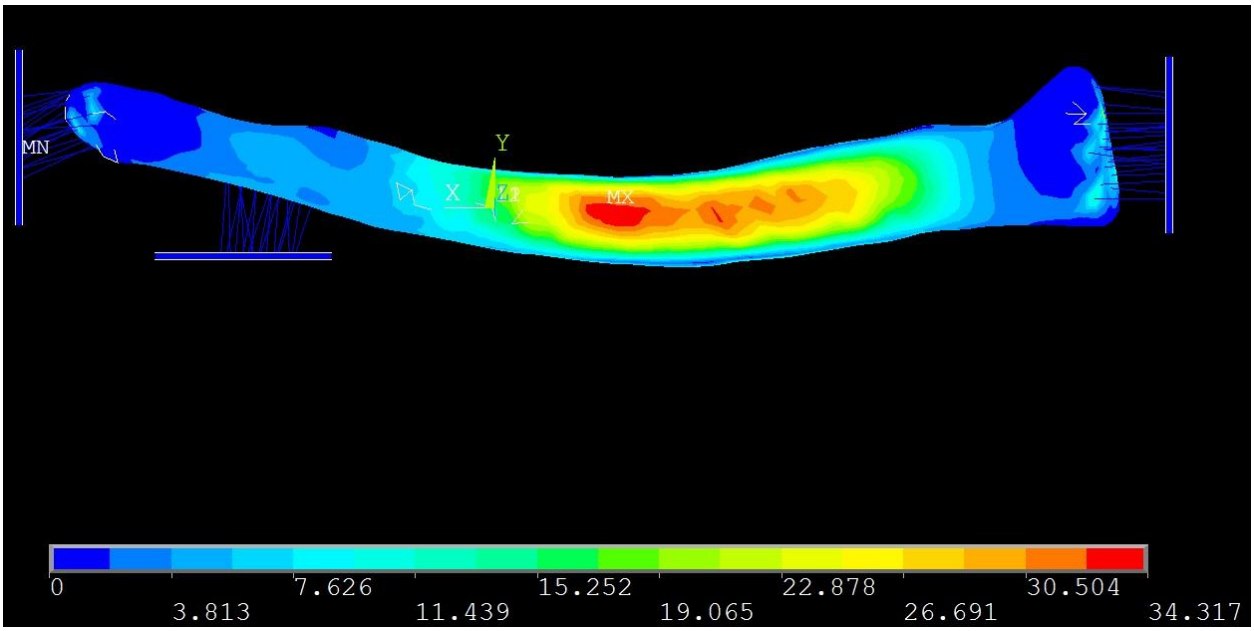

Figure 18: Back View of Stress Distribution of 135N Load Applied 38 mm from Sternoclavicular End

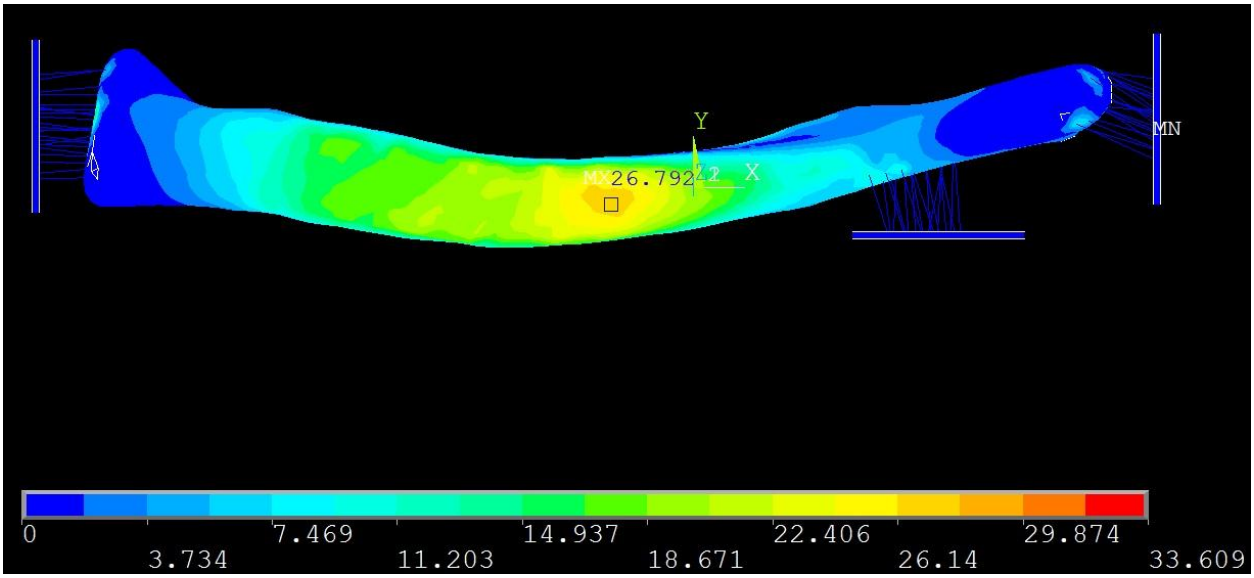

Figure 19: Front View of Stress Distribution of 135N Load Applied 63.5 mm from Sternoclavicular End

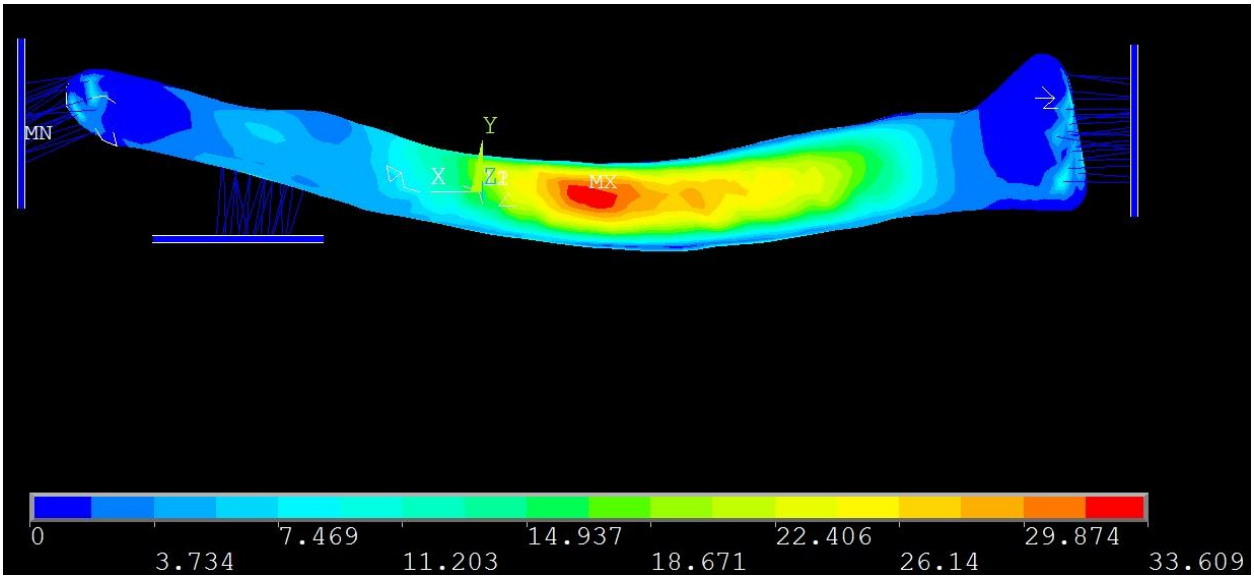

Figure 20: Back View of Stress Distribution of 135N Load Applied 63.5 mm from Sternoclavicular End

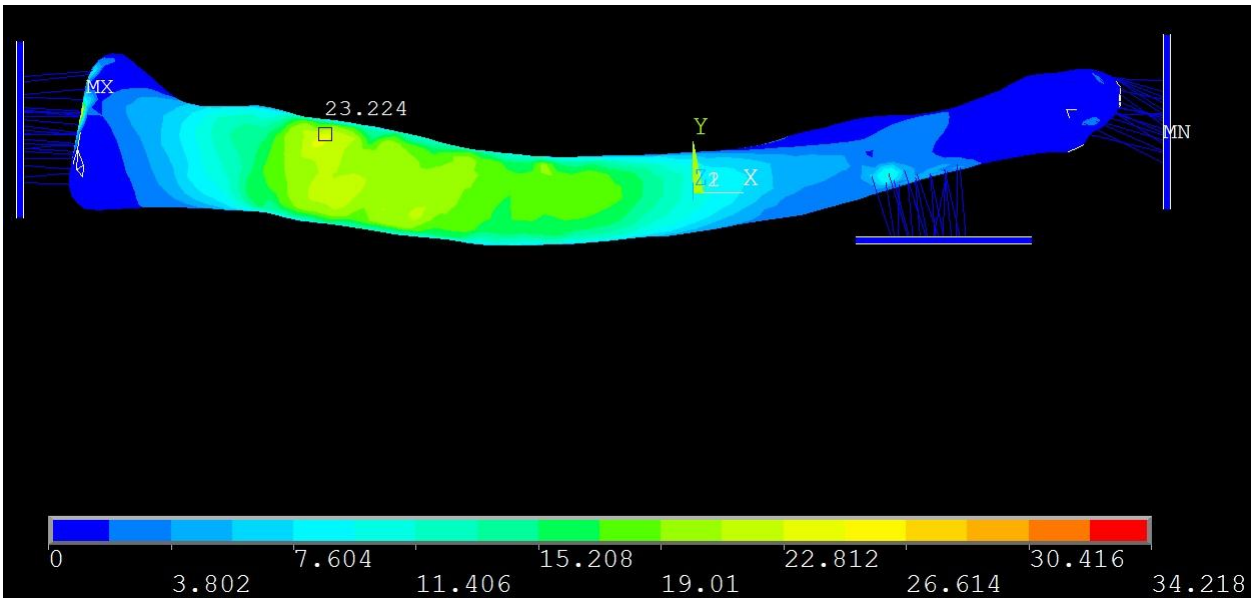

Figure 21: Front View of Stress Distribution of 135N Load Applied 13.5 mm from Sternoclavicular End

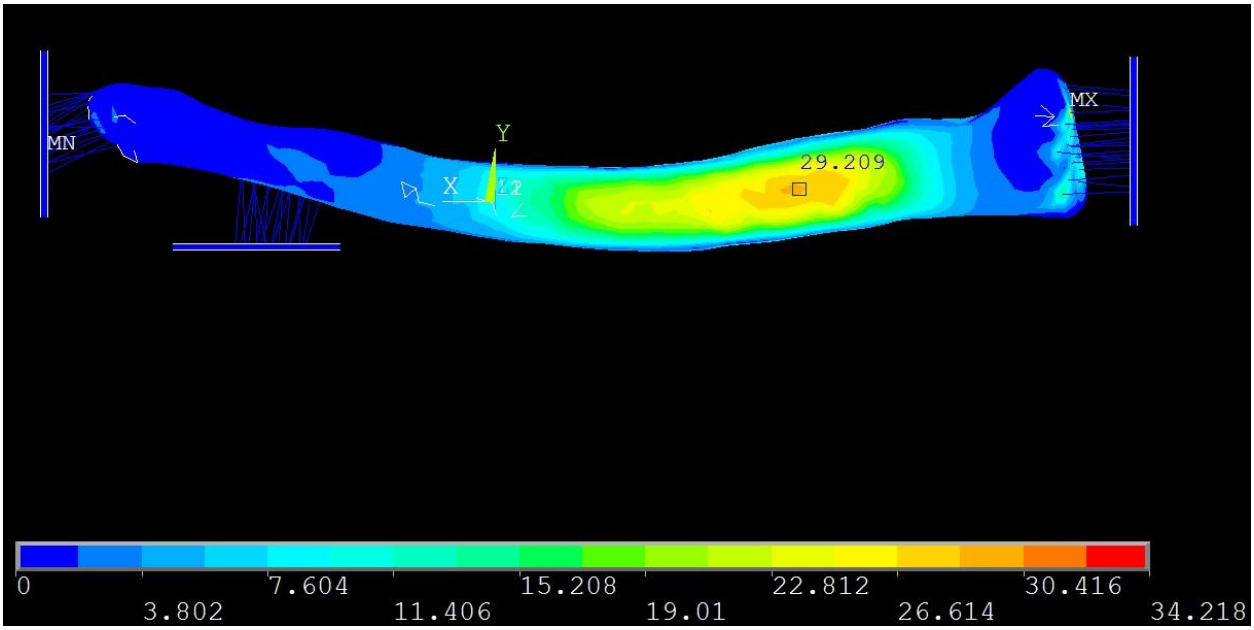

Figure 22: Back View of Stress Distribution of 135N Load Applied 13.5 mm from Sternoclavicular End

Chapter 4

4.1 Contributions

This research has helped to create a working model that will accurately represent a real human clavicle bone. Unlike the torso models in ATDs this model will be able to react to any load direction accurately rather than only a frontal or side load. This could aid in the development of improved physical models that could be placed in ATDs in order to obtain more accurate results from car crash testing.

4.2 Future Work

In the coming months the process that has been developed will be applied to modeling pediatric clavicles. A different finite element program may be used in order to perform dynamic force simulations.

One such program that may be considered is ABAQUS. There were a lot of issues with exporting the model from SolidWorks into ANSYS and different software that can create the mesh for the model may be looked into as well.

Using the models we can test the stresses that are a result of the force loads seen during a car crash. Force data obtained from a car crash reconstruction program MADYMO (MAthematical DYnamic MOdels) will be used as the input into the model. The results from these simulations will be compared with actual car crashes obtained from the Crash Injury Research and Engineering Network (CIREN) database. Figure 23 shows an example of the type of data listed from a car crash in the CIREN database. Using similar cases where there was a fracture of the clavicle and a control where there was not a fracture a fracture tolerance can be determined.

	Clavicle Injured Case	Control
CIREN ID:	470038879	470038846
Case Vehicle:	1992 GMC G2500 Vandura	1992 GMC G2500 Vandura
Vehicle Body Type:	Large van	Large van
PDOF:	0 degrees	0 degrees
CDC:	12FYAN7	12FYAN7
Total Delta V:	50 km/h	50 km/h
Case Occupant:	14 year old female	14 year old female
Height / Weight:	160 cm / 58 kg	157 cm / 52 kg
Seating Position:	Row 3 Right	Row 3 Left
Restraint:	Lap and shoulder belt; lap belt may have been worn on abodmen	Lap and shoulder belt; lap belt may have been worn on abodmen
Belt-Related Injury Decription:	R clavicle fracture	R chest skin abrasion
Other Significant Injuries:	Multiple L & R rib fxs; L lung lac and cont; liver, spleen, and kidney trauma	Liver and spleen lacs, pancreas cont

Figure 23: Example Car Crash Case from CIREN Database

References

Arbogast, K. B., Mong, D. A., Marigowda, S., Kent, R. W., Stacey, S., Mattice, J., et al. (2005). Evaluating Pediatric Abdominal Injuries. *19th International Technical Conference on the Enhanced Safety of Vehicles*, (pp. 1-15). Washington DC.

Bolte, J., Hines, M., McFadden, J., & Saul, R. (2000). Shoulder Response Characteristics and Injury Due to Lateral Glenohumeral Joint Impacts. *Stapp Car Crash Journal, 44*, 261-280.

Costic, R. S., Vangura Jr., A., Fenwick, J. A., Rodosky, M. W., & Debski, R. E. (2003). Viscoelastic Behavior and Structural Properties of the Coracoclavicular Ligaments. *Scandinavian Journal of Medicine & Science in Sports, 13*, 305-310.

Currey, J. D. (1979). Changes in the Impact Energy Absorption of Bone with Age. *Journal of Biomechanics, 12*, 459-469.

Currey, J. D., & Butler, G. (1975). The Mechanical Properties of Bone Tissue in Children. *The Journal of Bone and Joint Surgery*, 810-814.

Harrington Jr., M. A., Keller, T. S., Seiler III, J. G., Weikert, D. R., Moeljanto, E., & Schwartz, H. S. (1993). Geometric Properties and the Predicted Mechanical Behavior of Adult Human Clavicles. *Journal of Biomechanics, 26*, 417-426.

Harris, R. I., Wallace, A. L., Harper, G. D., Goldberg, J. A., Sonnabend, D. H., & Walsh, W. R. (2000). Structural Properties of the Intact and the Reconstructed Coracoclavicular Ligament Complex. *The American Journal of Sports Medicine, 28*, 103-108.

Hoyer, H. E., Kindt, R., & Lippert, H. (1980). Studies on the Biomechanics of the Human Clavicle. *Zeitschrift fur Orthopadie und ihre Grenzgebiete*, 915-922.

Kemper, A. R., Stitzel, J. D., Gabler, C., Duma, S. M., & Matsuoka, F. (2006). Biomechanical Response of the Human Clavicle Subjected to Dynamic Bending. *Biomedical Sciences Instrumentation* , 231-236.

Kemper, A. R., Stitzel, J. D., McNally, C., Gabler, H. C., & Duma, S. M. (2009). Biomechanical Response of the Human Clavicle: The Effects of Loading Direction on Bending Properties. *Journal of Applied Biomechanics, 25*, 165-174.

Nuckley, D. J., & Ching, R. P. (n.d.). Relationship Between Vertebral Bone Mineral Density and Strength.

Proubasta, I., & et al. (2002). Biomechanical Evaluation of Fixation of Clavicle Fractures. *Journal of the Southern Orthopaedic, 11(3)*, 148-152.

Skalak, R., & Chien, S. (1987). *Handbook of Bioengineering.* New York: McGraw-Hill.

Untaroiu, C. D., Duprey, S., Kerrigan, J., Li, Z., Bose, D., & Crandall, J. R. (2009). Experimental and Computational Investigation of Human Clavicle Response in Anterior-Posterior Bending Loading. *Biomedical Sciences Instrumentation*, 6-11.

Varghese, B. A., Miller, M. E., & Hangartner, T. N. (2008). Estimation of Bone Strength from Pediatric Radiographs of the Forearm. *Journal of Musculoskeletal and Neuronal Interactions, 8*, 379-390.

Vinz, H. (1972). Firmness of Pure Bone Substance: Approximate Method for the Determination of Bone Tissue Firmness Related to the Cavity-Free Cross Section. *Morphol Jahrb Gegenbaurs, 117*, 453-460.